

Synthesis, Spectroscopic Characterisation, and Metal Ion Interaction of a New α -Helical Peptide

Giuseppe Impellizzeri,* Giuseppe Pappalardo,* Roberto Purrello, Enrico Rizzarelli, and Anna Maria Santoro

Abstract: A 15-mer model peptide was synthesised by the solid phase method. The solution structure of this peptide was investigated by circular dichroism (CD) and NMR spectroscopy. CD results indicated that the peptide adopts a helical conformation in the presence of 2,2,2-trifluoroethanol (TFE) and its helicity is influenced by pH. NMR studies, carried out in H₂O/TFE (1:1), allowed the sequence-specific assignment of the

proton resonances to be made, in addition to a more precise location of the helical structure in the peptide sequence. The ability of different divalent metal ions (Cu²⁺, Ni²⁺) to induce an α -helix was also investigated in aqueous

solution by means of CD spectroscopy; the results obtained indicate that Ni²⁺ is able to promote the α -helical conformation at neutral pH. In contrast, the CD spectrum of the Cu²⁺-peptide complex does not show any indication of a helical conformation. The reasons for this behaviour are proposed on the basis of ESR and UV/Vis data.

Keywords: circular dichroism • helical structures • metal interactions • NMR spectroscopy • peptides

Introduction

Most of the regular secondary structures observed in folded proteins can be classified into three main motifs: α -helices, β -sheets and turns.^[1] Among these, the α -helix is the most abundant secondary structure element in proteins, and it is therefore of considerable importance to understand the factors that stabilise the α -helical structure, both in isolated fragments of proteins and in intact protein chains.^[2] The major advance in the field of peptide helices was the design of short peptide sequences that show good α -helix formation in water.^[3] Several studies have been aimed at promoting α -helix formation: i) by introducing conformational constraints in peptides,^[4] ii) by inserting α,α -substituted amino acids, such as α -aminoisobutyric acid in the peptidic sequence,^[5] iii) by the use of ion-pair interactions to stabilise the helix.^[3a, 6]

Another useful strategy is to direct the folding of an α -amino acid sequence and to stabilise existing secondary structures within polypeptides by metal complexation.^[7] For example, α -helical secondary structures have been stabilised by the formation of a metal-mediated cross-link that employs the side chains of both natural or unnatural amino acid residues located at the *i* and *i*+4 positions of the polypeptide sequence.^[8] The sequences, however, were carefully designed to display a helical structure in the absence of metal, and in a way such that small conformational changes caused by the addition of a metal could be easily detected. It would be interesting to investigate whether peptides which contain a greater number of metal-complexing amino acid side chains could be forced into stable helices by the presence of metal ions.

On the other hand, different metals tend to satisfy their own chemical and geometrical requirements upon complexation. Therefore, a peptide ligand might exhibit specific conformations in the presence of distinct metal ions. In this respect, we recently observed that divalent metal ions exhibit differing abilities to induce folding in a octapeptide containing histidine.^[7m] This differing ability has been correlated with the imidazole binding strength and the tendency to assume square-planar coordination by the metal ions studied. Interestingly, only Ni²⁺ is able to induce ordered peptide structures at pH 7.

In order to explore further the effect of metal complexation on the conformation of short oligopeptides, we have designed

[*] G. Impellizzeri, R. Purrello, E. Rizzarelli, A. M. Santoro
Dipartimento di Scienze Chimiche, Università di Catania
Viale A. Doria 6, 95125 Catania (Italy)
Fax: (+39)95 580138
E-mail: gimpellizzeri@dipchi.unict.it.

G. Pappalardo, E. Rizzarelli
Istituto per lo Studio delle Sostanze Naturali di Interesse Alimentare e Chimico Farmaceutico
Sezione per lo Studio di Modelli di Metallo-Enzimi del CNR
Viale A. Doria 6, 95125 Catania (Italy)
Fax: (+39)95-580138
E-mail: pappalardo@issn.ct.cnr.it

and synthesised the model peptide P¹D²A³D⁴A⁵H⁶A⁷H⁸A⁹H¹⁰A¹¹A¹²A¹³H¹⁴G¹⁵ (PADH).^[*] The peptide has been designed to produce a model with the propensity to adopt an α -helix conformation and, at the same time, has multiple sites for binding metals. The sequence contains a large number of alanine residues. Alanine was chosen because of its high propensity to form a helix.^[6c, 9] The Asp², His⁶ and Asp⁴, His⁸ residues were placed in position i , and $i+4$ respectively. In this position, an ion-pair or hydrogen bond interaction between their side chains might arise to stabilise the helical form. In addition, they are also well spaced for the simultaneous coordination to metal ions.^[8a,c] The remaining two histidine residues, namely His¹⁰ and His¹⁴, were inserted near the carboxyl termini of the sequence in order to maximise the benefits from the charge-helix dipole interaction,^[10] and were also in position i , and $i+4$ as a further site for the coordination of metal ions.^[8a,c] Proline was inserted as the first amino acid at

the N-terminus because of its ability to promote the first turn of an α -helix.^[1, 10]

Herein we report the structural characterisation of PADH by CD and NMR spectroscopy. Furthermore, the influence of Cu²⁺ and Ni²⁺ ions on the conformational behaviour of this peptide was investigated with CD, ESR and UV/Vis techniques.

Experimental Section

Materials: All *N*-fluorenylmethoxycarbonyl (Fmoc)-protected amino acids, Fmoc-Gly-Pepsyn-KA resin, 2-(1-*H*-benzotriazole-1-yl)-1,1,3,3-tetramethyluronium tetrafluoroborate (TBTU), *N*-hydroxybenzotriazole (HOBT) and *N,N*-dimethylformamide (DMF, peptide synthesis grade) were purchased from Millipore. *N,N*-Diisopropylethyl amine (DIEA) and triisopropylsilane were from Aldrich; 2,2,2-trifluoroethanol (TFE) was from Sigma; deuterated trifluoroethanol ([D₃]TFE) was from ICN; trifluoroacetic acid (TFA) was from Carlo Erba. All other chemicals were of the highest grade available and were used without further purification.

Peptide synthesis and purification: The peptide was synthesised on a Milligen Model 9050 peptide synthesiser, with Fmoc-Gly-Pepsyn-Ka as starting resin. All Fmoc-protected amino acids, except the proline residue, were introduced according to the TBTU/HOBT/DIEA method; the N-terminal proline residue was linked by the active ester method. The synthesis was carried out under a fourfold excess of amino acid at every cycle and each amino acid was recirculated through the resin for 40 minutes. The following amino acid derivatives were used: Fmoc-L-His(Trt)-OH, Fmoc-L-Ala-OH, Fmoc-L-Asp(OtBu)-OH, Fmoc-L-Pro-OPfp. After completion of the synthesis, the peptide was cleaved from the resin by treatment with a mixture of trifluoroacetic acid (TFA) and water which contained triisopropylsilane as a scavenger (TFA/H₂O/triisopropylsilane 95/2.5/2.5 v/v/v) for 1.5 h. The solution containing the free peptide was filtered off from the resin, concentrated in vacuo at a temperature not exceeding 30 °C and then precipitated with cold, freshly distilled ether. The precipitate was filtered and desiccated under vacuum to yield the crude peptide (190 mg). Purification of the peptide was accomplished by semipreparative reversed-phase HPLC on a Vydac C₁₈ (250 × 10 mm, particle size: 5 μm, pores: 300 Å) with a 35-min linear gradient of 5–20% acetonitrile/water/0.1% TFA with a flow rate of 3 mL min⁻¹. Elution profiles were monitored at 222 nm. The desired peptide fraction (20 min retention time) was collected, lyophilised and characterised by ¹H NMR spectroscopy and FAB-MS spectrometry (1448 [M+H]⁺, calcd 1447.63). Analytical RP-HPLC, performed on a Vydac C₁₈ (150 × 4.6 mm, particle size: 5 μm, pores: 300 Å) column with gradient mentioned above, indicated that the crude peptide was > 90% pure and the HPLC purified peptide > 98% pure.

pH measurements: All pH measurements were made with an Orion Model SA 520 pH meter equipped with a MI 410 combined pH electrode. The instrument was calibrated with standard buffers which had pH values of 4.01, 7.00 and 10.00. When pH measurements were run in the presence of TFE the electrode was calibrated just prior to use under the same experimental conditions.

Spectroscopic measurements:

CD spectroscopy: The CD spectra were obtained at 25 °C under a constant flow of nitrogen on a Jasco model J-600 spectropolarimeter which had been calibrated with an aqueous solution of ammonium D-camphorsulfate.^[11] The measurements reported were carried out in water, aqueous TFE, and at different pH values in a cuvette (1 mm path length). All experiments were performed in the UV region (190–250 nm). The spectra represent the average of 2–10 scans. CD intensities are expressed as mean residue ellipticities (deg cm² dmol⁻¹) calculated by $[\theta] = \theta/lcn$, where θ is the ellipticity observed (mdeg), l is the path length of the cell (cm), c is the peptide concentration (M) and n is the number of peptide bonds in the sequence.

NMR spectroscopy: Sample solutions were prepared in H₂O/D₂O (9:1 v/v) and in H₂O/[D₃]TFE (1:1 v/v) mixtures. The pH of the solutions were adjusted to 6.0 (value uncorrected for the isotope effect) by the addition of sodium hydroxide (0.1 M). Sodium (trimethylsilyl)propionate (TSP) was

[*] Abbreviations: one-letter symbols for the amino acids: P, Pro; D, Asp; A, Ala; H, His; G, Gly. CD, circular dichroism; DQF-COSY, double quantum-filtered correlation spectroscopy; TOCSY, total correlation spectroscopy; NOE, nuclear Overhauser effect; NOESY, nuclear Overhauser effect spectroscopy; ROESY, rotating-frame Overhauser effect spectroscopy; ESR electron spin resonance.

Abstract in Italian: *In questo lavoro è descritta la progettazione e la sintesi di un nuovo oligopeptide in grado di adottare una conformazione ad α -elica e di formare complessi con ioni metallici, attraverso la coordinazione con le catene laterali di residui ammino acidici inseriti in opportune posizioni della sequenza. Mediante l'utilizzo della spettroscopia CD è stato accertato che il peptide adotta una conformazione ad α -elica in presenza di TFE e che il suo grado di elicità è influenzato dal pH, indicando un coinvolgimento delle catene laterali ammino acidiche nella stabilizzazione dell'elica. Un dettagliato studio NMR, condotto in H₂O ed in presenza di TFE, ha permesso di attribuire tutti i segnali presenti nello spettro protonico ed una analisi più precisa sulla conformazione ad α -elica adottata dal peptide. Inoltre, la capacità dei differenti ioni metallici (Ni²⁺, Cu²⁺) di indurre la struttura ad α -elica è stata studiata per mezzo della spettroscopia CD. I risultati ottenuti indicano che il Ni²⁺ è in grado di promuovere la conformazione ad α -elica, mentre gli spettri CD ottenuti in presenza di Cu²⁺ non evidenziano la presenza di tale conformazione. Sulla base di indagini UV/Vis ed ESR condotti sui complessi formati dal peptide con i due metalli, si è concluso che la peculiare abilità del Ni²⁺ ad indurre la formazione di α -elica può essere spiegata con la formazione di complessi bidentati deboli che si formano presumibilmente con le catene laterali dell'istidina e dell'acido aspartico posti in posizione i , $i+4$; mentre il Cu²⁺ forma delle specie complesse più forti che causano il ripiegamento della catena polipeptidica attorno al centro metallico. I dati riportati nel presente lavoro possono assumere particolare importanza relativamente alla progettazione di biosensori di natura peptidica che mostrano selettività verso gli ioni metallici, ed inoltre contribuiscono ad aumentare le conoscenze sul ruolo svolto dagli ioni metallici nel folding delle proteine.*

added to the samples as a reference. The final concentration of the samples was ≈ 5 mM. 1D and 2D NMR spectra were recorded at room temperature on a Bruker AMX-600 spectrometer operating at 600.13 MHz. 1D NMR spectra were collected with 16 K data points over a spectral width of 6000 Hz in 64 scans. All 2D NMR spectra were obtained in the phase-sensitive mode with time-proportional phase incrementation (TPPI).^[12] DQF-COSY^[13] spectra were acquired with 2 K data points in the t_2 dimension and $2 \times 512 t_1$ increments, recording 8 transients for each increment. TOCSY^[14] spectra, were acquired with a MLEV-17 sequence of 63 ms and a mixing time of 68 ms with 2 K data points in the t_2 dimension and 512 t_1 increments, recording 32 transients for each increment. NOESY^[15] and ROESY^[16] spectra were collected with 2 K data points in the t_2 dimension and 512 t_1 increments recording 8 and 32 transients for each increment, respectively. A mixing time of 200 ms was used to obtain the NOESY spectrum, while ROESY spectra were performed at two different mixing times: 150 ms and 400 ms. The water resonance was suppressed by low-power presaturation. All the NMR spectra were processed with the software supplied by the manufacturer.

ESR spectroscopy: ESR spectra were recorded in frozen solutions on a Bruker ER200 D X-band instrument driven by the 3220 data system and with a standard low-temperature apparatus. The diphenylpicrylhydrazyl (DPPH) radical ($g = 2.0036$) was used to standardise the klystron frequency, the magnetic field was monitored by a Bruker type ER035 M gauss meter. Complex solutions (5 mM) were prepared by mixing aqueous solutions of isotopically pure $^{63}\text{Cu}(\text{NO}_3)_2 \cdot 6\text{H}_2\text{O}$ and peptide in a metal to ligand ratio of 1:1. Five solutions with pH values of 4, 5, 6, 7, and 8 were prepared in this way. After the pH was adjusted to the desired value, up to 5% methanol was added to increase the spectral resolution. All the measurements were carried out at 150 K.

UV/Vis spectroscopy: UV/Vis spectra were recorded on a Perkin–Elmer UV/Vis Lambda 2S spectrophotometer in cuvette with a path length of 2 cm and a sample concentration of 2 mM.

Results and Discussion

CD measurements: The ability of PADH to adopt the α -helix conformation was evidenced by CD spectroscopy; the CD spectrum of an α -helix consists of two minima at 222 nm and 206 nm, and a maximum at 193 nm.^[17] Because the random coil conformation has a very low ellipticity at 222 nm, the enhancement in the amount of helix present is represented by the increase of the intensity of the minimum at 222 nm. The CD spectra of PADH, collected in water and at various percentages of TFE in H_2O , are shown in Figure 1. TFE is

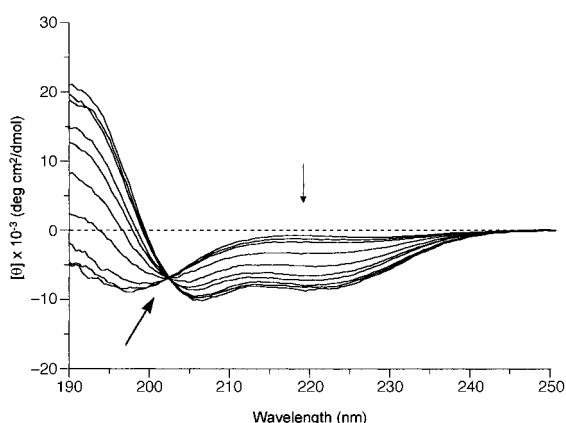


Figure 1. CD spectra of PADH at different percentages of TFE in water at 25 °C and pH 6.1. From top to bottom (thin arrow): 0, 5, 10, 20, 30, 40, 50, 60, 70, 80%. There is an apparent isodichroic point at about 203 nm (thick arrow).

known to induce helical conformation in peptides; however, the precise mechanism of this structure induction is still unknown. This induction is not general for all peptides and the propensity for helix formation has been suggested to be a prerequisite.^[18]

In the absence of TFE, the dominant CD feature is a strong negative band below 200 nm, indicative of a peptide with a predominantly random coil conformation.^[17] When CD spectra of PADH were measured in the presence of an increasing volume % of TFE in H_2O , a positive band emerged at about 190 nm, along with two negative bands centred at 206 and at 222 nm. The presence of an apparent isodichroic point near 203 nm, is indicative of the presence of a mixed helix–coil conformation.^[18c, 19] A plot of $[\theta]_{222}$ against TFE percentage (Figure 2) gives a sigmoidal curve, which indicates that the induction of the helical structure by TFE is a cooperative process.^[18c]

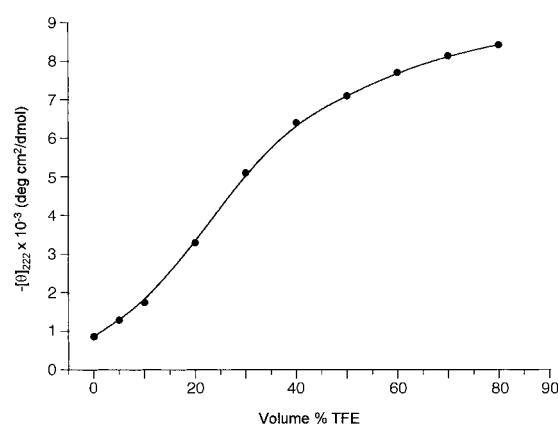


Figure 2. Plot of $[\theta]_{222}$ versus volume % TFE in H_2O for PADH under the same experimental conditions as Figure 1.

The measure of the $[\theta]_{222}$ is the most commonly used parameter to estimate the fraction of α -helix. However, it has been reported that although the $[\theta]_{222}$ value can be correctly applied to calculate the helix percentage in proteins, it fails in the estimation of the helix content in small peptides.^[20] Other spectral parameters can be considered to reveal helix propensity in small peptides: i) the $[\theta]$ ratio of the minimum at 222 nm to the minimum at a shorter wavelength, ii) the position of this last minimum, iii) the crossover wavelength λ_0 . In particular, an increase of the $[\theta]$ ratio to a value close to unity, together with a shift of the shorter wavelength minimum towards 206 nm and a shift of the λ_0 value to longer wavelengths are indicative parameters of high helix propensity. The above mentioned spectral parameters obtained from the spectra shown in Figure 1 are reported in Table 1. At $> 50\%$ TFE, the spectral parameters do not change significantly. This indicates that at this percentage of TFE, PADH is predominantly in the α -helix conformation.

Concentration-dependent CD studies were carried out at 25 °C in 50% TFE and at pH 7 (Figure 3). In the range of about 1–362 μM , the mean residue ellipticity $[\theta]_{222}$ is independent of the peptide concentration, indicating an intramolecular helical structure.^[6c]

Table 1. CD parameters of PADH in H₂O and at different volume % of TFE in H₂O.^[a]

% TFE	$[\theta]_{\min} \times 10^{-3}$ (λ_{\min} , nm)	$[\theta]_{222} \times 10^{-3}$	$[\theta]_{\text{ratio}}$	λ_0 [nm]	$[\theta]_{190} \times 10^{-3}$
0	-8.92 (197.6)	-0.87	0.10		-4.91
5	-8.43 (197.2)	-1.29	0.15		-4.59
10	-7.75 (198.8)	-1.75	0.22		-1.90
20	-6.67 (201.2)	-3.30	0.49	193.8	2.38
30	-7.49 (204.8)	-5.11	0.68	196.6	8.16
40	-8.20 (204.8)	-6.41	0.78	197.8	12.70
50	-8.64 (206.0)	-7.10	0.82	198.6	14.80
60	-9.38 (206.0)	-7.70	0.82	199.1	17.92
70	-9.63 (206.0)	-8.14	0.84	199.1	18.94
80	-10.12 (206.0)	-8.42	0.83	199.1	20.93

[a] Parameters are derived from the experimental CD spectra shown in Figure 1; $[\theta]$ is expressed as mean residue ellipticity ($\text{deg cm}^2 \text{dmol}^{-1}$) calculated as indicated in the Experimental Section; $[\theta]_{\text{ratio}}$ is the ratio of the ellipticity at 222 nm to that at the shorter wavelength minimum; λ_0 represents the wavelength at which the CD signal changes its sign.

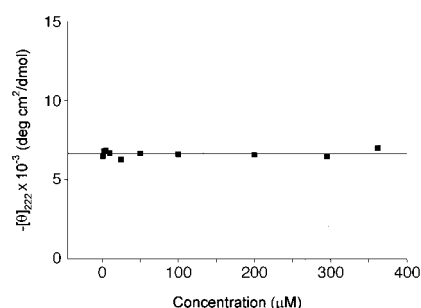


Figure 3. Dependence of the ellipticity at 222 nm on the concentration of PADH at 25 °C and in 50% TFE, pH 7. Each point represents the average of three determinations.

The effect of pH on helix formation has also been investigated both in water and in 50% aqueous TFE (Figure 4). The obtained data display a similar trend, indicating an increase in the ellipticity at 222 nm as the pH is raised. Some considerations can be made by analysing the curves. At pH 2.5, the peptide is completely protonated and, in this condition, exhibits the lowest helix content. As the pH is increased the ellipticity increases until a first plateau is reached at pH 7.5. Since the pK_a values of the aspartic acid and histidine side chains are expected to fall in this pH

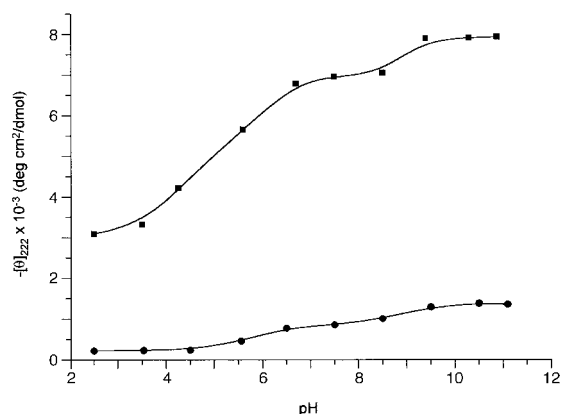


Figure 4. The pH dependence of the $[\theta]_{222}$ at 25 °C for PADH in 50% TFE/H₂O (■) and in pure H₂O (●).

range,^[21] it is reasonable to hypothesise that these amino acid residues influence the stabilisation of the α -helix conformation of PADH (this effect is particularly evident in the presence of TFE, see Figure 4). In particular, an increase in the amount of helix should result from the favourable interaction of the negatively charged carboxylate side chains of the aspartic acid residues with the helix dipole. This kind of ionic interaction is known to have a positive effect on the stabilisation of the helix structure.^[10] Additional stabilising contributions may arise from hydrogen bond or ion pair interactions between the carboxylate groups of the aspartic acid side chains and the imidazole side chains of the histidine residues located in positions i and $i+4$, respectively. The effects of the histidine residues are less interpretable because of their wide distribution along the sequence. We expect that the histidine residues located near the C-terminus (His¹⁰ and His¹⁴) should interact more strongly with the helix dipole when their imidazole side chains are protonated, on the other hand the histidine residues located at the interior positions (His⁶ and His⁸) should display opposite behaviour.^[10, 21b]

By raising the pH above 8.5, another increase in the helix content is observed and a final plateau is reached at pH \approx 10.5. This second increment is probably correlated with the deprotonation of the N-terminal amino group which results in a decrease in the electrostatic repulsion with the positive end of the helix macrodipole.^[22] Interestingly, in the case of the titration carried out in the presence of TFE, the effects of the charged groups on the helix structure are more evident. This different influence may simply be the consequence of the fact that PADH adopts an α -helix conformation in the TFE/H₂O mixture and this situation enhances the ionic effects; however, it also suggests that the ionic interactions could be strengthened, probably owing to the smaller dielectric constant of TFE compared to that of water.

NMR measurements:

¹H NMR resonance assignments: NMR studies were carried out both in H₂O and in [D₃]TFE/H₂O (1:1). Sequence-specific assignment was obtained by following the procedure described by Wüthrich.^[23] The sequential assignment of this peptide was not straightforward because of the redundancy of Ala and His residues in the central part of the sequence. This caused some difficulty, especially in the analysis of the spectra recorded in water, where the lack of a well-defined structure caused severe overlapping of the signals associated with the amide protons (Figure 5a). In the presence of TFE, the assignment became more manageable. Under these conditions, most of the degeneracy in the amide region was removed (Figure 5b) and a series of characteristic sequential NOEs were observed in both the NOESY and ROESY spectra. It is known that structured peptides show a greater dispersion of the amide resonances than their unstructured forms. The chemical shifts of the PADH protons recorded in [D₃]TFE/H₂O (1:1) are given in Table 2.

Analysis of secondary structure: Although CD spectroscopy represents the fastest way to verify helical conformation in peptides, it only gives a measure of the average amount of structure formed by the sample. On the other hand, NMR

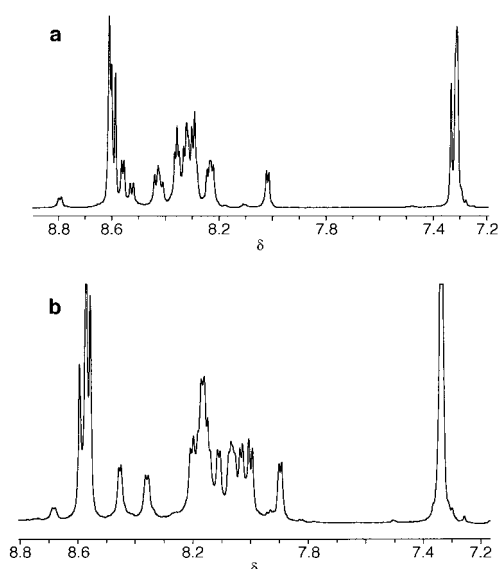


Figure 5. ¹H NMR spectrum of the NH/aromatic region of PADH dissolved in a) H₂O/D₂O (9:1) at pH 6 and in b) [D₃]TFE/H₂O (1:1) at pH 6.

Table 2. Proton chemical shifts of PADH.^[a]

Residue	NH	α -H	β -H	Others
Pro-1		4.42	2.10, 2.50	γ 2.10; δ 3.41, 3.50
Asp-2	8.68	4.78	2.80, 2.88	
Ala-3	8.45	4.29	1.44	
Asp-4	8.21	4.65	2.83	
Ala-5	8.14	4.18	1.45	
His-6	8.36	4.51	3.31	^[b]
Ala-7	8.05	4.23	1.46	
His-8	8.14	4.60	3.23, 3.35	^[b]
Ala-9	8.07	4.25	1.47	
His-10	8.17	4.65	3.23, 3.35	^[b]
Ala-11	8.11	4.31	1.45	
Ala-12	8.03	4.34	1.42	
Ala-13	7.90	4.30	1.40	
His-14	8.00	4.70	3.26, 3.38	^[b]
Gly-15	8.13	3.82, 3.97		

[a] Chemical shifts are expressed in δ and referenced to internal TSP [sodium(trimethylsilyl)propionate]. Values were measured in 50% [D₃]TFE and 50% H₂O at pH 6.1 and at 25 °C. [b] Sequence-specific assignment not obtained, the values are: 8.55, 8.57, 8.59, (2H); 7.34 (4H).

spectroscopy can define the extent and position of the helix in a given peptide more precisely.^[24] As seen above in the CD measurements, PADH is predominantly in the α -helical conformation in 50% TFE. Therefore, the conformational analysis was carried out in [D₃]TFE/H₂O (1:1). The presence of the helical conformation along the sequence was verified by applying four criteria of helicity: sequential and medium-range NOEs, values of ³J _{α N coupling constants and the values of the chemical shifts. It is known that the $d_{NN}(i, i+1)$ distance is shorter in the α -helix conformation than in an extended chain.^[23] A series of sequential $i, i+1$ amide–amide NOEs were clearly observed in both the NOESY and the ROESY spectra. When the same experiments}

were performed in water very few NOEs were observed in the same region; therefore, the presence of such NOEs in the spectra acquired in the presence of TFE is in agreement with a conformational transition toward a helical structure. A more stringent criterion for a α -helix structure is the presence of NOEs connecting α protons with β protons in the chain located three residues away.^[23] A series of successive $d_{\alpha\beta}(i, i+3)$ connectivities were observed and unambiguously assigned, starting from Ala⁵ up to His⁸. Additional cross-peaks may be present but are obscured by α,β cross-peaks belonging to the same residue, as in the case of Ala⁹–Ala¹², or their assignment is not univocal, as in the case of His¹⁰–Ala¹³ and Ala¹¹–His¹⁴ which are exchangeable with Asp⁴–Ala⁷ and Ala³–His⁶, respectively. Figure 6 summarises all the NOE connectivities observed between protons in the peptide, as well as several ³J _{α N coupling constants. The measured ³J _{α N coupling constants for the alanine residues are < 6 Hz, which suggests that these residues tend to adopt a helical conformation, while those pertinent to the histidine residues are bigger, according to their lesser ability in stabilising the helical structure.^[21b]}}

It is well known that in α -helical peptides, the α -proton chemical shifts tend towards upfield values.^[25] A convenient way to detect these variations in the chemical shifts is to plot the differences between the measured value and the respective random coil value versus the position along the peptide sequence (Figure 7). The negative values for adjacent H α protons from residue Ala³ to Ala⁹ indicate the presence of a helical structure in this section of the peptide backbone. This evidence is also in good agreement with the $d_{\alpha\beta}(i, i+3)$ NOEs observed in the same region of the sequence. The histidines located near the C-terminus tend to interrupt the propagation of the helical conformation notwithstanding the contrary effect of the intervening three alanines. When all the above-mentioned criteria are applied, it is possible to state that the peptide adopts a significant amount of helical structure in 50% aqueous TFE. This observation is in agreement with the CD data.

Figure 8 shows the MM+ energy-minimised structure of the proposed conformation adopted by PADH in

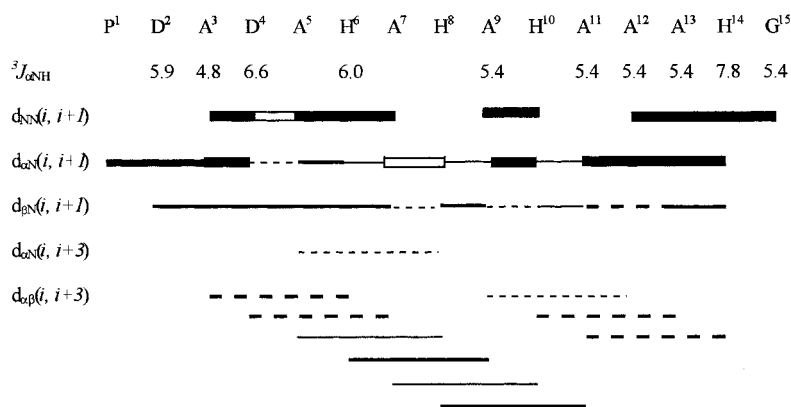


Figure 6. Schematic summary of the NOE connectivities and $J(\text{NH}, C_{\alpha}\text{H})$ coupling constants of PADH observed in [D₃]TFE/H₂O (1:1). Solid lines indicate unambiguous NOEs. Empty and dashed lines indicate possible NOEs where chemical shift degeneracy interferes with identification. Line thickness is proportional to the NOE intensity. The amino acid residues are indicated by the standard one-letter code.

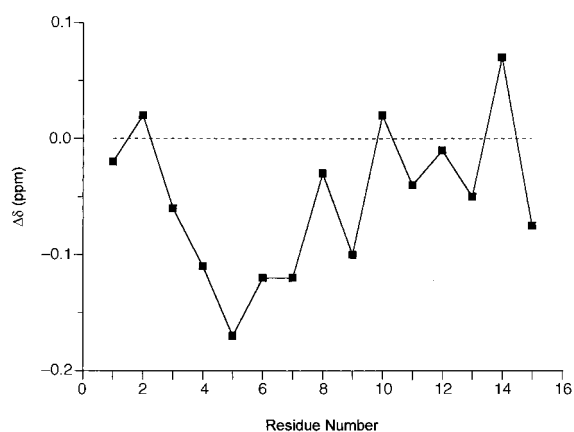


Figure 7. Plot of the difference between the observed chemical shifts of $C_{\alpha}H$ protons of PADH in $[D_3]TFE/H_2O$ (1:1) and those of random coil values ($\Delta\delta = \delta_{obs} - \delta_{random\ coil}$) versus the position along the sequence. The random coil values were taken from Wüthrich.^[23]

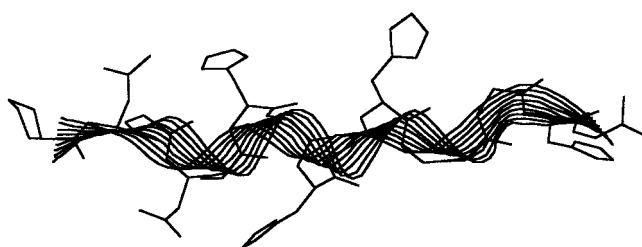


Figure 8. Molecular mechanics-optimised structure of the possible helical conformation adopted by PADH. For the sake of clarity, the hydrogen atoms and the alanine side chains have been omitted. The peptide backbone is presented as a ribbon.

50% TFE/ H_2O . This structure was obtained by transforming the measured $^3J_{\alpha N}$ coupling constants into dihedral angles, and the values obtained were then introduced as constraints into the calculation. Moreover, interproton distance restraints were generated from the ROESY and NOESY data. The obtained structure is a distorted, somewhat elongated helical conformation.

Interaction with metal ions: The influence of Cu^{2+} and Ni^{2+} ions on the PADH conformation was investigated by CD, ESR and UV/Vis techniques. Figure 9 shows the CD spectra obtained in the absence (spectrum I) and in the presence of Ni^{2+} at pH 7 (spectra II and III). The CD spectrum recorded at a Ni^{2+} :PADH ratio of 5:1 (spectrum III) shows an inflection of the minimum at 222 nm accompanied by the shift of the other minimum towards higher wavelengths and by the presence of a cross-over. These spectral features suggest a conformational transition towards a helical structure. Evidence for the complexation of Ni^{2+} with PADH was provided by UV/Vis experiments. The spectra were recorded at pH 6, because the presence of a precipitate at pH 7 prevented the measurements. The electronic spectra, recorded in the visible region at Ni^{2+} :PADH ratios of 1:1 and 2:1, show a shift of the characteristic bands of Ni^{2+} to higher frequencies. In particular, with regard to the spectroscopic data obtained for the hexaquo ion under the same experimental conditions, the

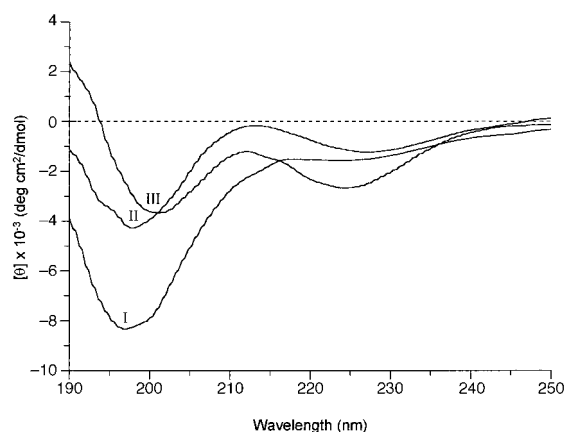


Figure 9. CD spectra of PADH ($3.2 \times 10^{-4} M$) in the absence (I) and in the presence of Ni^{2+} with Ni^{2+} :PADH ratios of 1:1 (II) and 5:1 (III) in H_2O at pH 7.

$^3T_{2g}(F) \leftarrow ^3A_{2g}(F)$ transition shifts from 8870 cm^{-1} to 10340 cm^{-1} , while the $^3T_{1g}(F) \leftarrow ^3A_{2g}(F)$ transition shifts from 14500 cm^{-1} to 14840 cm^{-1} (this second transition is split into two components, therefore the centre of these two bands has been taken as the indicative value) (see Table 3). When the

Table 3. EPR and UV/Vis parameters of Ni^{2+} and Cu^{2+} complexes formed with PADH.

Metal/ligand ratio	pH	g_{\parallel}	A_{\parallel} (10^4 cm^{-1})	λ_1 [nm] (ϵ [$\text{dm}^3\text{ mol}^{-1}\text{ cm}^{-1}$])	λ_2 [nm] (ϵ [$\text{dm}^3\text{ mol}^{-1}\text{ cm}^{-1}$])
$[Ni(H_2O)_6]^{2+}$	6.0	–	–	1149 (0.7)	690 (1.8)
	1:1	6.0	–	966 (7.1)	674 (9.5)
	2:1	6.0	–	966 (6.9)	674 (9.1)
	3:1	6.0	–	966 (4.1)	682 (6.4)
	5:1	6.0	–	–	687 (5.6)
Cu^{2+}	1:1	4.0	2.295(3) 180(4)	614 (95)	–
	1:1	7.0	2.229(3) 189(3)	594 (205)	–

Ni^{2+} :PADH ratio was increased from 3:1 to 5:1 the visible spectrum became more complicated because of the extra spectral contributions due to the free Ni^{2+} hexaquo ion. This suggests that PADH is able to accommodate up to two Ni^{2+} ions in its structure. In the spectra obtained in with metal:ligand ratios of 1:1 and 2:1, negligible variations are observed, which indicates that the two ions are located in quite similar binding sites. Moreover, the shifts are significantly low, when compared to the signals of the hexaquo ion, thus suggesting that the donor atoms involved in the interaction with the two Ni^{2+} ions form weak complexes. On the basis of these data, it is possible to hypothesise that each Ni^{2+} is complexed with the side chains of one aspartyl and one histidyl residues in position $i, i+4$, as represented in Figure 10.

The effects of Cu^{2+} on the peptide conformation are very different than those observed for the Ni^{2+} ion. Figure 11 shows the CD spectra recorded at pH 4 in the absence (spectrum I) and at different Cu^{2+} :PADH ratios (spectra II and III). The spectra obtained in the presence of Cu^{2+} do not show any features of a helical structure, but rather resemble that of a random coil. Information concerning the copper binding site

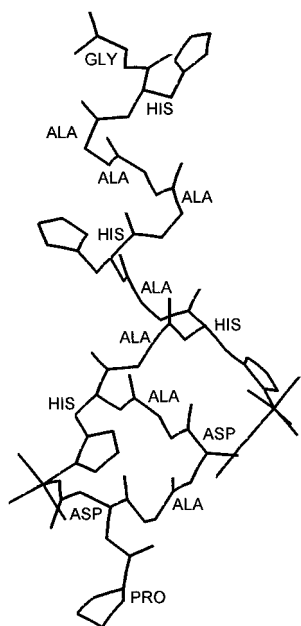


Figure 10. Sketch of the optimised structure of the PADH–Ni²⁺ complex. The hydrogen atoms and the alanine side chains are not shown for the sake of clarity.

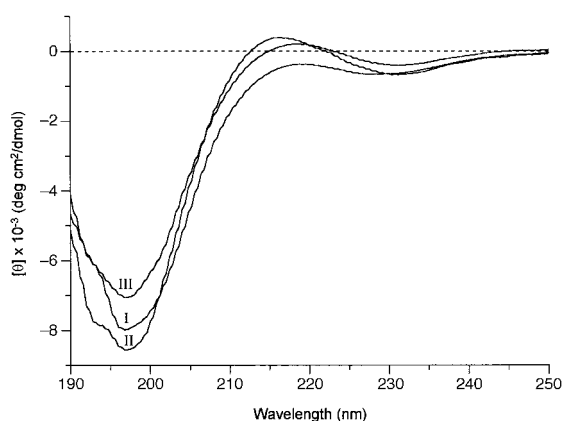


Figure 11. CD spectra of PADH (3.6×10^{-4} M) in the absence (I) and in the presence of Cu²⁺ with Cu²⁺:PADH ratios of 1:1 (II) and 5:1 (III) in H₂O at pH 4.

was obtained with ESR and UV/Vis investigations. The ESR spectra of frozen solutions of the ⁶³Cu²⁺–PADH system showed magnetic parameters which changed according to the pH of the aqueous solution (Table 3). The spectrum obtained at pH 4 showed magnetic parameters somewhat similar to those determined in the case of [Cu(imidazole)₄]²⁺ species,^[26] but the slightly different g_{\parallel} and A_{\parallel} values can be associated with an arrangement of the four donor atoms in a plane distorted towards a tetrahedral coordination. Unfortunately, it was not possible to ascertain the number of nitrogen atoms coordinated to Cu²⁺ because the spectrum did not show any s.h.f. (superhyperfine) pattern. Therefore, the probability that one or two carboxylate oxygen atoms participate in the coordination cannot be ruled out. Nevertheless, whichever donor atoms are involved in the complexation, they lead to the formation of a single complex species, as observed in the

ESR spectrum, that does not induce helical conformation, as evidenced in the CD spectra. If the pH of the aqueous solution was raised to 7–8, g_{\parallel} decreased and A_{\parallel} increased as a consequence of the deprotonation of amide nitrogen atoms which can substitute for the imidazole nitrogen atoms or the carboxylate oxygen atoms. This trend is also confirmed by visible optical data since on raising the pH a blue shift of the copper absorption band is clearly observed.^[27] The CD spectra recorded at pH 7 do not show the presence of any helical structure either (not shown).

The data obtained with Ni²⁺ and Cu²⁺ metals point out an interesting aspect since it seems to indicate that PADH adopts different conformations with respect to the metal ion. In other model peptides^[8] different metal ions influence, in a positive or a negative fashion, the stabilisation of the α -helix, by complexing with a single designed metal binding site. In the present case, the metal ion has several sites along the peptide sequence to choose from; therefore each metal might impose its preferred coordination geometry giving rise to different peptide conformations. In this respect, the observation that Ni²⁺ forms weak two-coordinate complexes with the amino acid side chains could explain its peculiar capability of inducing the helical structure in PADH, whereas the propensity of Cu²⁺ to form more stable four-coordinate complex species forces the peptide to fold around the metal centre.

Conclusions

We have designed and synthesised a new model peptide in which amino acid residues, such as Asp and His, were introduced in appropriate positions along the sequence in order to sustain helical conformation and to permit complexation to a metal ion. On the basis of the CD and NMR data, it is possible to confirm that the peptide is predominantly in α -helix conformation in 50% H₂O/TFE solution. Moreover, the pH dependence of helix formation in PADH indicates that the protonation states of Asp and His residues, as well as those relative to the N- and C-terminus, are important determinants of the observed helicity. The analysis of NMR data suggests that the helix conformation includes mainly the seven residues at the N-terminus (from Ala³ to Ala⁹), while the remaining two histidines located near the C-terminus appear to prevent the propagation of the helix in this direction.

The conformational properties of PADH upon complexation with different metal ions, were found to depend on the type of metal utilised; in particular, when PADH is complexed with Ni²⁺ at pH 7 a helical structure is present. In contrast, the presence of Cu²⁺ at pH 4 did not induce the helix structure.

In conclusion, we have demonstrated that PADH retains a good propensity to helix formation and that its conformation can be modulated by metal complexation. We believe that the results reported herein could be of importance for the construction of metal-complexing macromolecular systems that adopt different three-dimensional structures depending on the type of metal ion utilised.

Acknowledgments: We thank the CNR (Rome) for partial financial support. We also thank Prof. I. Bertini (University of Florence-Servizio

Nazionale di Risonanza Magnetica Nucleare) for the NMR facilities. We are grateful to Miss T. Campagna for recording CD and ESR spectra.

Received: February 11, 1998 [F1003]

- [1] J. S. Richardson, D. C. Richardson in *Prediction of Protein Structure and the Principles of Protein Conformation* (Ed.: G. D. Fasman) Plenum, New York and London, **1989** pp. 1–98.
- [2] a) T. E. Creighton, *Proteins*, Freeman and Company, New York, **1984**; b) D. J. Barlow, J. M. Thornton, *J. Mol. Biol.* **1988**, *201*, 601–608; c) G. D. Fasman, in ref. [1], pp. 193–316; d) J. M. Scholtz, R. L. Baldwin, *Annu. Rev. Biophys. Biomol. Struct.* **1992**, *21*, 95–118.
- [3] a) S. Marqusee, R. L. Baldwin, *Proc. Natl. Acad. Sci. USA* **1987**, *84*, 8898–8902; b) S. Marqusee, V. H. Robbins, R. L. Baldwin, *ibid.* **1989**, *86*, 5286–5290.
- [4] a) A. Ravi, B. V. V. Prasad, P. Balam, *J. Am. Chem. Soc.* **1983**, *105*, 105–109; b) G. Ösapay, J. W. Taylor, *ibid.* **1990**, *112*, 6046–6051; c) D. Y. Jackson, D. S. King, J. Chmielewski, S. Singh, P. G. Schultz, *ibid.* **1991**, *113*, 9391–9392; d) M. Chorev, E. Roubini, R. L. McKee, S. W. Gibbons, M. E. Goldman, M. P. Caulfield, M. Rosenblatt, *Biochemistry* **1991**, *30*, 5968–5974; e) G. Ösapay, J. W. Taylor, *J. Am. Chem. Soc.* **1992**, *114*, 6966–6973; f) C. Bracken, J. Gulyas, J. W. Taylor, J. Baum, *ibid.* **1994**, *116*, 6431–6432; g) H. Mihara, K. Tomizaki, N. Nishino, T. Fujimoto, H. Tamaoki, Y. Kobayashi, *Biopolymers* **1994**, *34*, 963–967; h) J. C. Phelan, N. J. Skelton, A. C. Braisted, R. S. McDowell, *J. Am. Chem. Soc.* **1997**, *119*, 455–460.
- [5] a) B. V. V. Prasad, P. Balam, *CRC Crit. Rev. Biochem.* **1984**, *16*, 307–348; b) G. R. Marshall, E. E. Hodgkin, D. A. Langs, G. D. Smith, J. Zabrocki, M. T. Leplawy, *Proc. Natl. Acad. Sci. USA* **1990**, *87*, 487–491; c) I. L. Karle, R. B. Rao, S. Prasad, R. Kaul, P. Balam, *J. Am. Chem. Soc.* **1994**, *116*, 10355–10361, and references therein.
- [6] a) A. Bierzynski, P. S. Kim, R. L. Baldwin, *Proc. Natl. Acad. Sci. USA* **1982**, *79*, 2470–2474; b) P. C. Lyu, L. A. Marky, N. R. Kallenbach, *J. Am. Chem. Soc.* **1989**, *111*, 2733–2734; c) P. C. Lyu, M. I. Liff, L. A. Marky, N. R. Kallenbach, *Science* **1990**, *250*, 669–673; d) G. Merutka, E. Stellwagen, *Biochemistry* **1991**, *30*, 1591–1594; e) P. J. Gans, P. C. Lyu, M. C. Manning, R. W. Woody, N. R. Kallenbach, *Biopolymers* **1991**, *31*, 1605–1614; f) E. Stellwagen, S. Park, W. Shalongo, A. Jain, *ibid.* **1992**, *32*, 1193–1200; g) J. M. Scholtz, H. Qian, V. H. Robbins, R. L. Baldwin, *Biochemistry* **1993**, *32*, 9668–9676.
- [7] a) T. Handel, W. F. DeGrado, *J. Am. Chem. Soc.* **1990**, *112*, 6710–6711; b) J. T. Kellis, Jr., R. J. Todd, F. H. Arnold, *Bio/Technol.* **1991**, *9*, 994–995; c) R. J. Todd, M. E. Van Dam, D. Casimiro, B. L. Haymore, F. H. Arnold, *Proteins: Struct. Funct. Genet.* **1991**, *10*, 156–161; d) S. Suh, B. L. Haymore, F. H. Arnold, *Protein Eng.* **1991**, *4*, 301–305; e) M. Lieberman, T. Sasaki, *J. Am. Chem. Soc.* **1991**, *113*, 1470–1471; f) M. R. Ghadiri, C. Soares, C. Choi, *ibid.* **1992**, *114*, 825–831; g) M. R. Ghadiri, C. Soares, C. Choi, *ibid.* **1992**, *114*, 4000–4002; h) M. R. Ghadiri, M. A. Case, *Angew. Chem.* **1993**, *105*, 1663–1667; *Angew. Chem. Int. Ed. Engl.* **1993**, *32*, 1594–1597; i) T. Sasaki, M. Lieberman, *Tetrahedron* **1993**, *49*, 3677–3689; j) R. P. Cheng, S. L. Fisher, B. Imperiali, *J. Am. Chem. Soc.* **1996**, *118*, 11349–11356; m) R. P. Bonomo, L. Casella, L. De Gioia, H. Molinari, G. Impellizzeri, T. Jordan, G. Pappalardo, R. Purrello, E. Rizzarelli, *J. Chem. Soc. Dalton Trans.* **1997**, 2387–2389.
- [8] a) M. R. Ghadiri, C. Choi, *J. Am. Chem. Soc.* **1990**, *112*, 1630–1632; b) F. Ruan, Y. Chen, P. B. Hopkins, *ibid.* **1990**, *112*, 9403–9404; c) M. R. Ghadiri, A. K. Fernholz, *ibid.* **1990**, *112*, 9633–9635; d) F. Ruan, Y. Chen, K. Itoh, T. Sasaki, P. B. Hopkins, *J. Org. Chem.* **1991**, *56*, 4347–4354.
- [9] a) P. Y. Chou, G. D. Fasman, *Adv. Enzymol.* **1978**, *47*, 45–148; b) K. T. O'Neil, W. F. DeGrado, *Science* **1990**, *250*, 646–650; c) S. Padmanabhan, S. Marqusee, T. Ridgeway, T. M. Laue, R. L. Baldwin, *Nature* **1990**, *344*, 268–270; d) M. Blaber, X. Zhang, B. W. Matthews, *Science* **1993**, *260*, 1637–1640.
- [10] a) D. E. Blagdon, M. Goodman, *Biopolymers* **1975**, *14*, 241–245; b) J. S. Richardson, D. C. Richardson, *Science* **1988**, *240*, 1648–1652; c) S. Dasgupta, J. A. Bell, *Int. J. Pept. Protein Res.* **1993**, *41*, 499–511.
- [11] G. C. Chen, J. T. Yang, *Anal. Lett.* **1977**, *10*, 1195–1207.
- [12] D. Marion, K. Wüthrich, *Biochem. Biophys. Res. Commun.* **1983**, *113*, 967–974.
- [13] M. Rance, O. W. Sørensen, G. Bodenhausen, G. Wagner, R. R. Ernst, K. Wüthrich, *Biochem. Biophys. Res. Commun.* **1983**, *117*, 479–485.
- [14] A. Bax, D. G. Davis, *J. Magn. Reson.* **1985**, *65*, 355–360.
- [15] J. Jeener, B. H. Meier, P. Bachmann, R. R. Ernst, *J. Chem. Phys.* **1979**, *71*, 4546–4553.
- [16] A. Bax, D. G. Davis, *J. Magn. Reson.* **1985**, *63*, 207–213.
- [17] G. Holzwarth, P. Doty, *J. Am. Chem. Soc.* **1965**, *87*, 218–228.
- [18] a) S. I. Segawa, T. Fukuno, K. Fujiwara, Y. Noda, *Biopolymers* **1991**, *31*, 497–509; b) H. J. Dyson, G. Merutka, J. P. Waltho, R. A. Lerner, P. E. Wright, *J. Mol. Biol.* **1992**, *226*, 795–817; c) A. Jasanoff, A. R. Fersht, *Biochemistry* **1994**, *33*, 2129–2135.
- [19] M. E. Holtzer, A. Holtzer, *Biopolymers* **1992**, *32*, 1589–1591.
- [20] a) S. Vuilleumier, M. Mutter, *Biopolymers* **1993**, *33*, 389–400; b) F. Nastro, A. Lombardi, G. Morelli, O. Maglio, G. D'Auria, C. Pedone, V. Pavone, *Chem. Eur. J.* **1997**, *3*, 340–349.
- [21] a) J. Sancho, L. Serrano, A. R. Fersht, *Biochemistry* **1992**, *31*, 2253–2258; b) K. M. Armstrong, R. L. Baldwin, *Proc. Natl. Acad. Sci. USA* **1993**, *90*, 11337–11340; c) B. M. P. Huyghues-Despointes, J. M. Scholtz, R. L. Baldwin, *Protein Sci.* **1993**, *2*, 1604–1611; d) H. V. Joshi, M. S. Meier, *J. Am. Chem. Soc.* **1996**, *118*, 12038–12044.
- [22] R. Fairman, K. R. Shoemaker, E. J. York, J. M. Stewart, R. L. Baldwin, *Proteins Struct. Funct. Genet.* **1989**, *5*, 1–7.
- [23] K. Wüthrich, *NMR of Proteins and Nucleic Acids*, Wiley, New York **1986**.
- [24] M. I. Liff, P. C. Lyu, N. R. Kallenbach, *J. Am. Chem. Soc.* **1991**, *113*, 1014–1019.
- [25] a) A. Pardi, G. Wagner, K. Wüthrich, *Eur. J. Biochem.* **1983**, *137*, 445–454; b) A. Pastore, V. Saudek, *J. Magn. Reson.* **1990**, *90*, 165–176; c) D. S. Wishart, B. D. Sykes, F. M. Richards, *FEBS Lett.* **1991**, *293*, 72–80; d) D. S. Wishart, B. D. Sykes, F. M. Richards, *J. Mol. Biol.* **1991**, *222*, 311–323; e) D. S. Wishart, B. D. Sykes, F. M. Richards, *Biochemistry* **1992**, *31*, 1647–1651; f) J. Rizo, F. J. Blanco, B. Kobe, M. D. Bruch, L. M. Gierasch, *ibid.* **1993**, *32*, 4881–4894.
- [26] R. P. Bonomo, F. Riggi, A. J. Di Bilio, *Inorg. Chem.* **1988**, *27*, 2510–2512.
- [27] J. P. Laussac, A. Robert, R. Haran, B. Sarkar, *Inorg. Chem.* **1986**, *25*, 2760–2765.